SCIENTIFIC REPORTS

OPEN

SUBJECT AREAS:
CONDENSED-MATTER PHYSICS
OPTICAL MATERIALS AND STRUCTURES
OPTICAL PHYSICS
NANOSCALE MATERIALS

Received
6 March 2013

Accepted
8 March 2013

Published
27 March 2013

Correspondence and requests for materials should be addressed to Z.W.P. (panz@uga.edu)

Photostimulated near-infrared persistent luminescence as a new optical read-out from Cr^{3+}-doped $LiGa_5O_8$

Feng Liu[1,2], Wuzhao Yan[1,2], Yen-Jun Chuang[1], Zipeng Zhen[3], Jin Xie[3] & Zhengwei Pan[1,2]

[1]College of Engineering, University of Georgia, Athens, GA 30602, USA, [2]Department of Physics and Astronomy, University of Georgia, Athens, GA 30602, USA, [3]Department of Chemistry, University of Georgia, Athens, GA 30602, USA.

In conventional photostimulable storage phosphors, the optical information written by x-ray or ultraviolet irradiation is usually read out as a visible photostimulated luminescence (PSL) signal under the stimulation of a low-energy light with appropriate wavelength. Unlike the transient PSL, here we report a new optical read-out form, photostimulated persistent luminescence (PSPL) in the near-infrared (NIR), from a Cr^{3+}-doped $LiGa_5O_8$ NIR persistent phosphor exhibiting a super-long NIR persistent luminescence of more than 1,000 h. An intense PSPL signal peaking at 716 nm can be repeatedly obtained in a period of more than 1,000 h when an ultraviolet-light (250–360 nm) pre-irradiated $LiGa_5O_8$:Cr^{3+} phosphor is repeatedly stimulated with a visible light or a NIR light. The $LiGa_5O_8$:Cr^{3+} phosphor has promising applications in optical information storage, night-vision surveillance, and *in vivo* bio-imaging.

When a storage phosphor is exposed to high-energy radiation, such as x-ray or ultraviolet (UV) light, part of the excitation energy is stored in the phosphor by capturing charge carriers (electrons or holes) in traps which are generally lattice defects or impurities[1–3]. The stored energy can then be liberated by thermal, optical or other physical stimulations, resulting in stimulated emissions from the emitting centers in the phosphors. Storage phosphors, especially the thermally stimulated storage phosphors whose energy is released upon heating (including the thermal energy available at room temperature) based on thermoluminescence[4–8] and photostimulable storage phosphors whose energy is released by low-energy light (photon) illumination based on photostimulated luminescence (PSL; also called as optically stimulated luminescence, OSL)[1,2,9–12], have found a plethora of important applications, e.g., as self-sustained night-vision luminescent materials and in the fields of dosimetry and x-ray imaging.

The photostimulable storage phosphors exhibiting PSL phenomenon can act as excellent imaging plates for optical information write-in and read-out. The optical information write-in and read-out processes require optically illuminating the phosphor plate twice. The first exposure by an x-ray beam or a UV light "writes" a latent image in the form of trapped electrons on the phosphor plate. The number of trapped electrons is proportional to the amount of radiation absorbed locally and the latent image is optically readable within a certain time frame (usually within 8 h for practical use) after the exposure. The second illumination with a light of appropriate wavelength, typically with an intense light with low energy (e.g., red He-Ne lasers), "reads" the image in the form of higher energy visible PSL signal (e.g., violet-blue emission for BaFBr:Eu^{2+} phosphor[10,11]). Most of the trapped electrons are extracted during the read-out process, and the residual electrons remaining on the phosphor plate can be erased through illumination with bright fluorescent light so that the plate can be used again. Therefore, the photostimulable storage phosphors which exhibit the PSL phenomenon can be used as erasable and rewritable optical memory media for many advanced optical storage applications. For example, the best-known and the most commercially successful photostimulable storage phosphor so far is BaFBr:Eu^{2+}, which is being widely used as the imaging plates in computed radiography[10,11].

Here we report a new optical read-out form, photostimulated persistent luminescence (PSPL) in the near-infrared (NIR), from a Cr^{3+}-doped $LiGa_5O_8$ NIR persistent phosphor[13]. An Intense PSPL signal with an emission peaking at 716 nm can be repeatedly obtained in a period of more than 1,000 h when a UV light (250–360 nm) pre-irradiated $LiGa_5O_8$:Cr^{3+} phosphor is repeatedly stimulated by a light between 380–1,000 nm.

Results

Photoluminescence and super-long persistent luminescence in the NIR. Cr^{3+}-doped $LiGa_5O_8$ was studied in the 1970s but neither NIR persistent luminescence nor NIR PSPL was reported[14]. Figure 1a shows the normalized

photoluminescence emission and excitation spectra of a $LiGa_5O_8:Cr^{3+}$ phosphor disc at room temperature. Under excitation at 400 nm, the material exhibits a narrow-band emission peaking at 716 nm. This NIR emission is characteristic of Cr^{3+} ions and can be attributed to the spin-forbidden $^2E \rightarrow {}^4A_2$ transition. The associated broad background emission ranging from ~650 nm to ~850 nm originates mostly from the phonon sidebands of the $^2E \rightarrow {}^4A_2$ transition[14]. The photoluminescence excitation spectrum monitored at 716 nm emission covers a very broad spectral region (from ~250 to ~660 nm) and consists of three main excitation bands originating from the inner transitions of Cr^{3+}, including the 300 nm band originating from the $^4A_2 \rightarrow {}^4T_1(^4P)$ transition, the 415 nm band originating from the $^4A_2 \rightarrow {}^4T_1(^4F)$ transition, and the 605 nm band originating from the $^4A_2 \rightarrow {}^4T_2(^4F)$ transition.

Besides the intense NIR photoluminescence, the excitation of UV light can also induce very-long-lasting NIR persistent luminescence in $LiGa_5O_8:Cr^{3+}$ phosphor with a persistence time >1,000 h (here the persistence time is defined as the duration for which an eye can see with the aid of a night-vision goggle in a dark room[8]; see Supplementary Information). Figure 1b shows the persistent luminescence decay curve of a $LiGa_5O_8:Cr^{3+}$ phosphor disc monitored at 716 nm after irradiation by 300 nm UV light for 20 min. The recording lasted for 120 h. As can be seen, the persistent luminescence intensity drops quickly in the first several hours and then decays slowly. After 120 h of persistent emission, the persistent luminescence intensity is still significantly high, indicating that the NIR persistent luminescence should last much longer than 120 h. The persistent luminescence intensities of the $LiGa_5O_8:Cr^{3+}$ phosphor disc at 10 min and 1 h after ceasing the excitation were estimated to be ~4.7 mW m^{-2} and ~1.2 mW m^{-2}, respectively (Supplementary Information and Supplementary Fig. S1). The upper inset of Fig. 1b shows a persistent luminescence emission spectrum recorded at 1 h after the stoppage of the 300 nm UV light irradiation. The profile of the persistent luminescence emission spectrum is almost identical to that of the photoluminescence emission spectrum (Fig. 1a), indicating that the NIR persistent luminescence originates

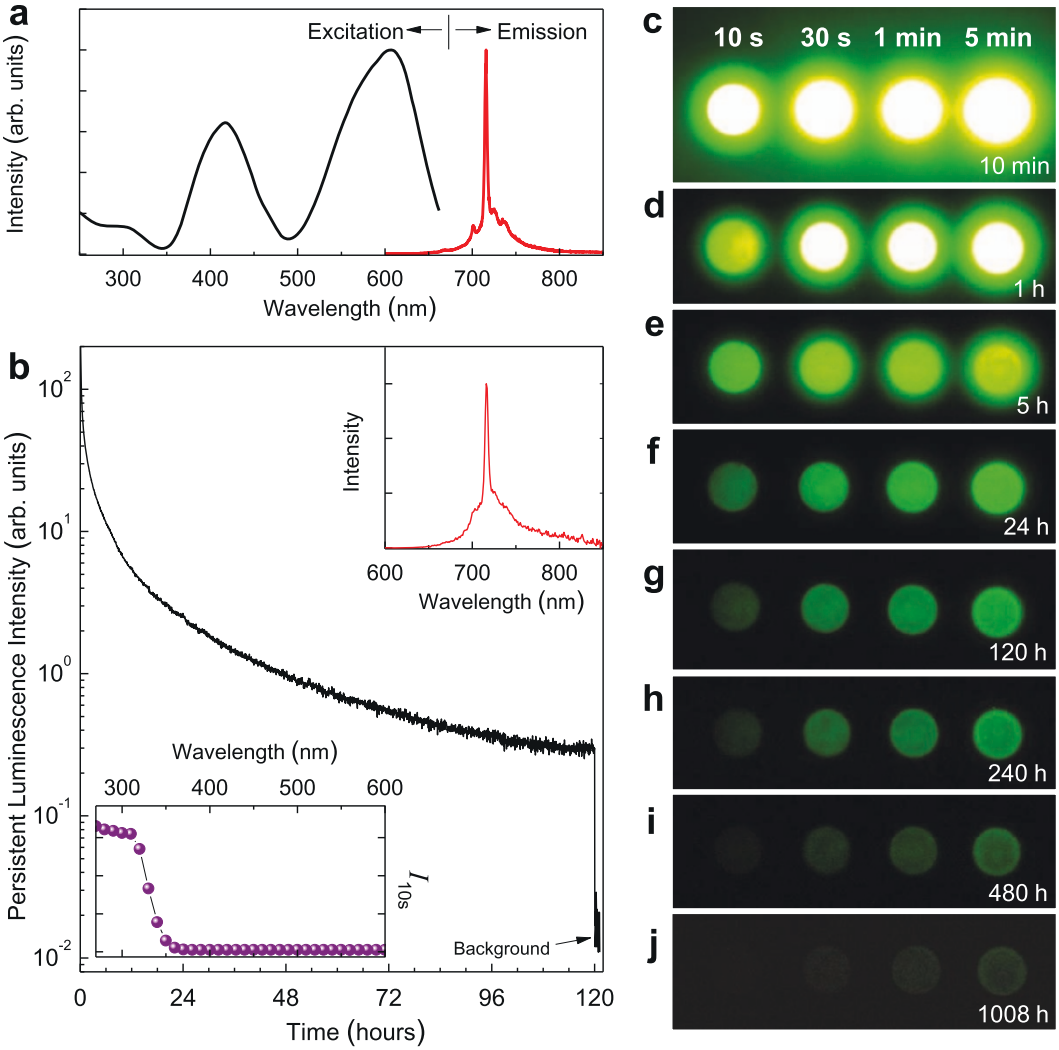

Figure 1 | Photoluminescence and persistent luminescence of $LiGa_5O_8:Cr^{3+}$ phosphor discs at room temperature. (a) Normalized excitation and emission spectra for photoluminescence. The emission spectrum is acquired under 400 nm light excitation and the excitation spectrum is obtained by monitoring 716 nm emission. (b) NIR persistent luminescence decay curve monitored at 716 nm after irradiation by 300 nm light for 20 min. The upper inset shows the persistent luminescence emission spectrum recorded at 1 h after the stoppage of the irradiation. The bottom inset is the persistent luminescence excitation spectrum obtained by plotting the persistent luminescence intensity (I_{10s}) monitored at 716 nm as a function of the excitation wavelengths over the 250–600 nm spectral range. The disc was irradiated for 5 min at each measured wavelength using a xenon arc lamp. (c–j) NIR images of four phosphor discs taken at different persistent luminescence times (10 min to 1,080 h) after irradiated by a 254 nm lamp for 10 s to 5 min. The imaging parameters are: (c–f) manual/ISO 400/10 s, (g–i) manual/ISO 800/30 s, and (j) manual/ISO 1600/30 s.

from the Cr^{3+} emitting centers. However, unlike the NIR photoluminescence which can be effectively excited by a wide range of wavelengths (~250–660 nm) (Fig. 1a), the NIR persistent luminescence in $LiGa_5O_8:Cr^{3+}$ cannot be induced by low-energy visible light irradiation. To evaluate the effectiveness of different excitation wavelengths (energies) for persistent luminescence, we measured the persistent luminescence decay curves monitored at 716 nm after the excitation of monochromatic light with different wavelengths between 250–600 nm in 10 nm steps (Supplementary Fig. S2), recorded the persistent luminescence intensity at 10 s after the stoppage of each excitation (I_{10s}), and plotted the intensity I_{10s} as a function of the excitation wavelengths, as the ball curve shown in the bottom inset of Fig. 1b. It is clear that the NIR persistent luminescence can be effectively achieved by UV irradiation between 250–360 nm (250 nm is the low limit of the xenon emission in the FluoroLog-3 spectrofluorometer), and the effectiveness increases as the excitation moves to shorter wavelengths.

The very-long-lasting NIR persistent luminescence of the $LiGa_5O_8:Cr^{3+}$ phosphor discs was also visually evaluated using a night-vision monocular in a dark room. Figure 1c–j shows the changes of NIR emission "brightness" with a decay time up to 1,008 h for four $LiGa_5O_8:Cr^{3+}$ discs after exposure to a 4 W 254 nm UV lamp for 10 s, 30 s, 1 min and 5 min. Figure 1c–j clearly shows that the $LiGa_5O_8:Cr^{3+}$ phosphor discs can be effectively activated by the 254 nm UV lamp and seconds to minutes of UV irradiation can result in 1,008 h of persistent NIR emission. It should be noted that, as the PSPL phenomenon that will be discussed below, the energy stored in the material during excitation is not completely released even after 1,008 h room-temperature decay. Thus, the actual persistent luminescence decay time of the $LiGa_5O_8:Cr^{3+}$ phosphor should be longer than 1,008 h.

Photochromism. In irradiating the $LiGa_5O_8:Cr^{3+}$ phosphor discs using a 254 nm UV lamp in room light environment, we observed that the body color of the $LiGa_5O_8:Cr^{3+}$ sample changed from greenish to reddish, as the digital pictures shown in Figs. 2a and 2b. This UV irradiation induced coloration phenomenon is long-lived at room temperature, lasting for more than one month (the samples need to be stored in the dark); however, it can be quickly bleached by external stimulations, such as through illumination with bright fluorescent light or through heating at around 400°C. This coloration/bleaching process can be repeatedly carried out without leaving any permanent changes to the optical performance of the $LiGa_5O_8:Cr^{3+}$ samples. The change of body color due to UV irradiation is qualitatively reflected by measuring the diffuse reflectance absorption on the samples with and without UV irradiation, as the spectra shown in Fig. 2c. Compared with the non-irradiated sample (curve 3), the spectra of the UV-irradiated sample (curves 1 and 2) contain an additional green absorption band peaking at ~500 nm, as the dash-line curve and dot-dash-line curve shown in Fig. 2c. The presence of the additional green absorption band, together with the strong absorption of the material to blue light, make the UV-irradiated $LiGa_5O_8:Cr^{3+}$ discs appear to be reddish in room light condition.

Since the repetitive coloration/bleaching processes do not cause permanent change to the samples, the coloration phenomenon can be attributed to the formation of photochromic centers[15,16], which may result from the trapping of photogenerated electrons by the deep-level lattice defects (such as oxygen vacancies adjacent to the chromium ions) in $LiGa_5O_8:Cr^{3+}$. Also, since the fading of coloration is accompanied by the decrease of persistent luminescence intensity at room temperature, the deep-level lattice defects used to form the photochromic centers may also act as deep electron traps responsible for the long persistent luminescence. To further understand the properties of electron traps and photochromic centers in $LiGa_5O_8:Cr^{3+}$, we conducted thermoluminescence measurements

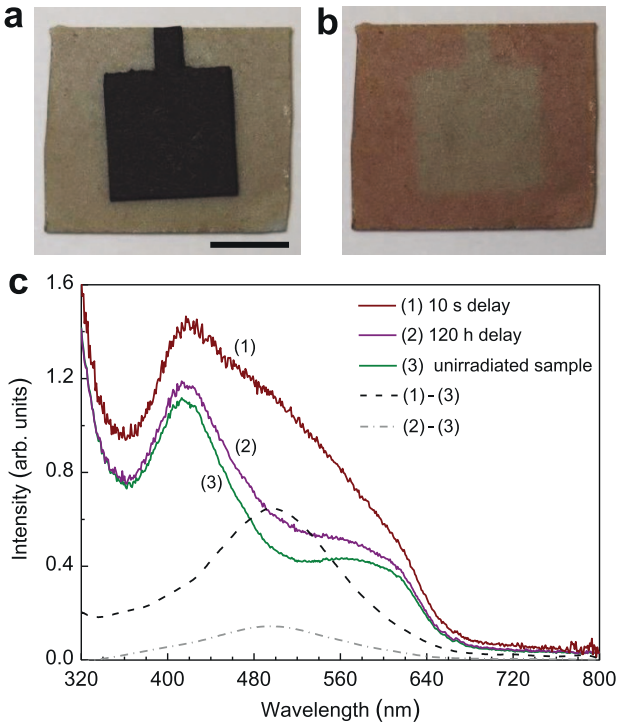

Figure 2 | UV-irradiation-induced coloration and changes in diffuse reflectance absorption of $LiGa_5O_8:Cr^{3+}$ phosphor plates. (a) Digital image of a 15 × 15 mm^2 $LiGa_5O_8:Cr^{3+}$ phosphor plate with its center covered by an 8 × 8 mm^2 black paper in room light environment. Scale bar, 5 mm. (b) The same plate as the one in (a) after exposed to a 254 nm UV lamp for 5 min. The paper was removed after the irradiation. (c) Diffuse reflectance absorption spectra acquired on $LiGa_5O_8:Cr^{3+}$ plates with and without UV irradiation. Curve 1 and curve 2 were recorded on a 300 nm-light-irradiated plate (for 20 min) with delay times of 10 s and 120 h, respectively. Curve 3 was acquired on a bleached plate (without UV pre-irradiation). The dash-line curve is the difference between curve 1 and curve 3. The dot-dash-line curve is the difference between curve 2 and curve 3.

on phosphor discs undergoing different delay times, as shown in Fig. 3a. The dot-dash-line curve in Fig. 3a shows the thermoluminescence curve acquired immediately (delay time, 10 s) after the stoppage of 300 nm light irradiation (for 20 min). The curve consists of two broad bands with maxima at 150°C and 220°C, which correspond to the shallow and deep traps, respectively. When the delay time increases to 120 h (the solid-line curve in Fig. 3a), a majority of the shallow-trap band disappears and the deep-trap band still exists, indicating that it is the deep traps that are responsible for the super-long persistent luminescence at room temperature. Since the photo-stimulation method has been frequently used to study the photochromic centers in storage phosphors[2], we then conducted photostimulated thermoluminescence measurements on the decayed $LiGa_5O_8:Cr^{3+}$ samples. The dash-line curve in Fig. 3a shows the thermoluminecence curve of a 120 h-decayed $LiGa_5O_8:Cr^{3+}$ disc after being exposed to 400 nm illumination for 100 s. Compared with the 120 h-decayed sample without photostimulation, the 400 nm-light stimulation significantly changes the thermoluminescence curve profile, i.e., the deep-trap band intensity decreases while the shallow-trap band reappears. This means that after the 400 nm-light photostimulation, some of the electrons in the deep traps are photo-released and the emptied shallow traps are refilled. (Note that the phenomenon of electron transfer from deep traps to shallow traps under external stimulation was also recently observed in some mechanoluminescent materials[17,18]).

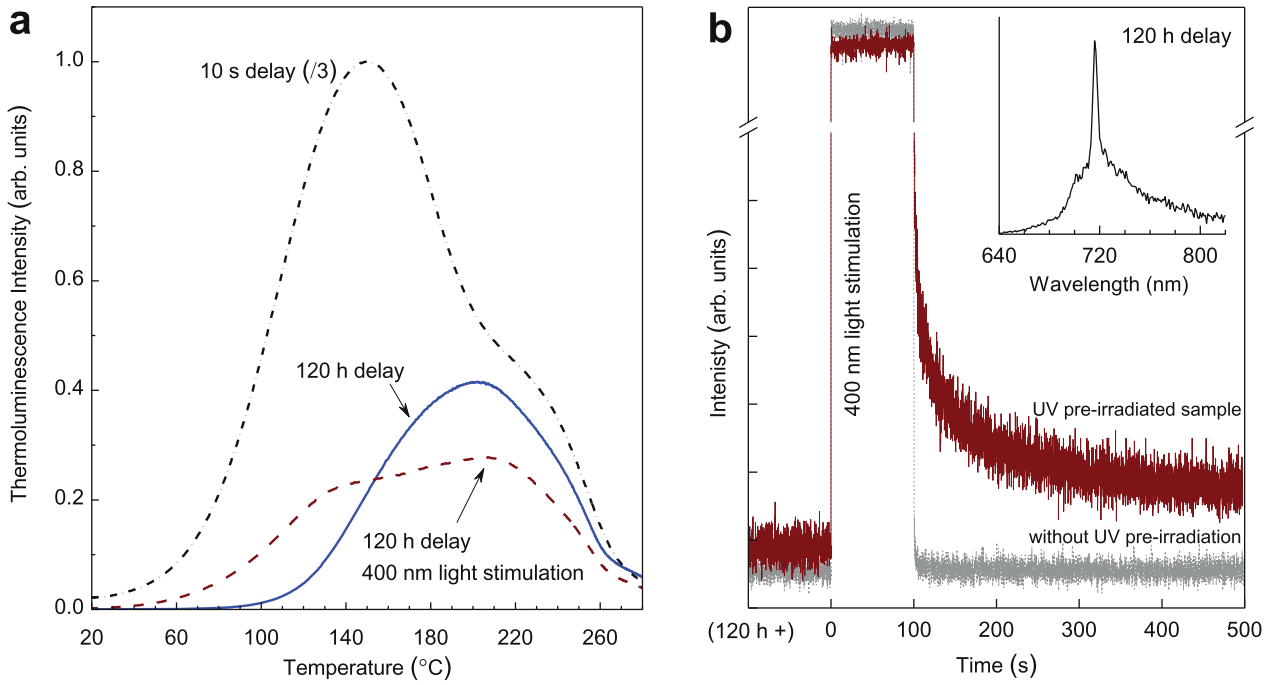

Figure 3 | Thermoluminescence spectra and PSPL decay curves of $LiGa_5O_8:Cr^{3+}$ phosphor discs. (a) Thermoluminescence curves monitored at 716 nm emission over 20–280°C. The samples were pre-irradiated by 300 nm UV light for 20 min. The dot-dash-line curve and solid-line curve were acquired at delay times of 10 s and 120 h, respectively. The dash-line curve was acquired on a 120 h-decayed disc after stimulation by 400 nm light for 100 s. (b) PSPL decay curves monitored at 716 nm. The brown curve was acquired on a 120 h-decayed disc (pre-irradiated by 300 nm light for 20 min), while the grey curve was recorded on a bleached disc (without UV pre-irradiation). The inset is the PSPL emission spectrum of the 120 h-decayed disc, which was recorded at 10 s after the stoppage of the stimulation. The wavelength of the stimulation light is 400 nm.

Photostimulated persistent luminescence (PSPL). The photostimulation induced electron trap redistribution, especially the refill of the shallow traps, suggests that photostimuation can affect the persistent luminescence behaviors of the UV pre-irradiated $LiGa_5O_8:Cr^{3+}$ phosphor. To verify this assumption, we illuminated a 120 h-decayed $LiGa_5O_8:Cr^{3+}$ disc with 400 nm light for 100 s and measured its persistent luminescence decay curve (monitored at 716 nm), as the brown curve shown in Fig. 3b. Figure 3b clearly shows that the 400 nm light illumination increases the persistent luminescence intensity and thus a new PSPL phenomenon occurs. For comparison, we also conducted the same measurement on a completely bleached (i.e., without UV pre-irradiation) $LiGa_5O_8:Cr^{3+}$ disc, as the grey curve shown in Fig. 3b. No persistent luminescence was observed in the bleached sample after the 400 nm light illumination, which is consistent with the persistent luminescence excitation spectrum shown in the bottom inset of Fig. 1b. The inset of Fig. 3b is the PSPL emission spectrum of the 120 h-decayed disc, which was recorded at 10 s after the stoppage of the stimulation. The profile of the PSPL emission spectrum is almost identical to that of the photoluminescence emission spectrum (Fig. 1a) and the persistent luminescence emission spectrum (upper inset of Fig. 1b).

The NIR PSPL phenomenon in $LiGa_5O_8:Cr^{3+}$ is analogous to the visible PSL in conventional photostimulable storage phosphors, indicating that the $LiGa_5O_8:Cr^{3+}$ phosphor has the potential to be used as a new type of erasable and rewritable optical memory media for optical information write-in and read-out. For the measurement in Fig. 3b, the write-in and read-out sources are 300 nm UV light and 400 nm visible light, respectively. To precisely determine the range of write-in and read-out energies needed for the NIR PSPL in $LiGa_5O_8:Cr^{3+}$, we plotted PSPL write-in and read-out spectra by measuring PSPL decays over a wide range of wavelengths between 250–660 nm. In plotting the PSPL write-in spectrum, we irradiated a bleached $LiGa_5O_8:Cr^{3+}$ disc using monochromatic UV light between 250–380 nm in 10 nm steps and recorded the persistent luminescence decay curves with and without a 400 nm light stimulation, as shown by the three sets of representative curves in Fig. 4a. We defined the PSPL intensity as the difference between the persistent luminescence intensities of each set of decays with and without photostimulation at the time of 10 s after the stoppage of the stimulation, as indicated by the vertical double arrowheads in Fig. 4a. The PSPL write-in spectrum was then obtained by plotting the PSPL intensities as a function of the write-in wavelengths (250–380 nm), as the ball curve shown on the left panel of Fig. 4c. The write-in spectrum reveals that in order to induce NIR PSPL in $LiGa_5O_8:Cr^{3+}$, the write-in wavelength should be shorter than 360 nm and within the measured wavelengths of 250–360 nm the shorter the excitation wavelength the more effective the write-in process is. Moreover, by comparing Fig. 4c with the bottom inset of Fig. 1b, it can be found that the PSPL write-in spectrum is identical in shape to the persistent luminescence excitation spectrum even though they were obtained by different methods and their physical meanings are different (The PSPL write-in spectrum shows the energy required to fill the deep traps, i.e., to form the photochromic centers, while the persistent luminescence excitation spectrum reveals the energy needed to photoionize the localized electrons from Cr^{3+} to the conduction band[8]). The coincidence of these two spectra clearly indicates that the filling of the deep traps (i.e., the formation of the photochromic centers) accompanies the photoionization of Cr^{3+} in $LiGa_5O_8$.

In acquiring the PSPL read-out spectrum, the write-in wavelength was fixed at 300 nm, while the read-out wavelengths were tuned between 380–660 nm in 10 nm steps. Using the same method as above, we acquired PSPL decay curves and plotted the PSPL read-out spectrum, as shown in Fig. 4b and on the right panel of Fig. 4c, respectively. The read-out spectrum reveals that the PSPL phenomenon can be induced by the entire visible spectrum and that the shorter the stimulation wavelength the more effective the read-out

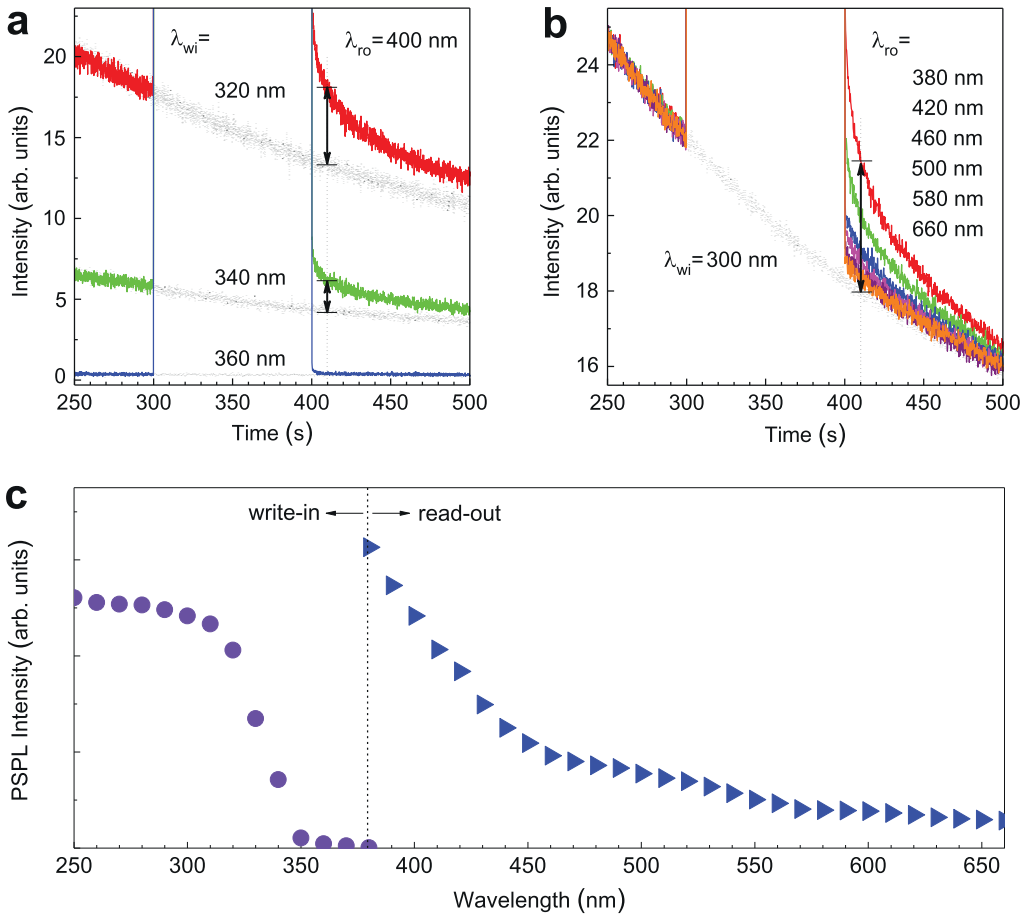

Figure 4 | Optical write-in and read-out spectra for PSPL in $LiGa_5O_8:Cr^{3+}$. (a) Persistent luminescence decay curves monitored at 716 nm with (colored solid-line curves) and without (grey dash-line curves) photostimulation. The write-in wavelengths (λ_{wi}) are 320 nm, 340 nm and 360 nm. The read-out wavelength (λ_{ro}) is 400 nm. (b) Persistent luminescence decay curves monitored at 716 nm with (colored solid-line curves) and without (grey dash-line curve) photostimulation. The write-in wavelength (λ_{wi}) is 300 nm. The read-out wavelengths (λ_{ro}) vary between 380 nm and 660 nm. For the measurements in (a) and (b), the read-out process (i.e., stimulation) starts at 5 min after ceasing the write-in process (i.e., UV pre-irradiation). The vertical double arrowheads in (a) and (b) represent the PSPL intensities. (c), PSPL write-in spectrum (the ball curve in left panel) and read-out spectrum (the triangle curve in right panel) plotted according to the data from (a) and (b), respectively.

process is. Moreover, our read-out experiments further showed that the energy stored in the $LiGa_5O_8:Cr^{3+}$ phosphor can also be read out by NIR light stimulation, such as a 980 nm NIR laser, as the PSPL decay curve shown in Supplementary Fig. S3. Thus, our read-out experiments reveal that unlike the visible PSL phenomenon in conventional photostimulable phosphors in which the read-out wavelength is longer than the emission wavelength, the stimulation wavelength for the NIR PSPL in $LiGa_5O_8:Cr^{3+}$ phosphor can be either shorter or longer than the emission wavelength.

It is worth noting from Fig. 4c that there is no overlap between the PSPL write-in and PSPL read-out spectra in the $LiGa_5O_8:Cr^{3+}$ phosphor. This is important because while the visible light is reading the optical information written by the UV light, it does not write new information into the material. In addition, the very broad write-in and read-out spectra allow one to easily find suitable optical sources, such as inexpensive laser diodes and light emitting diodes (LEDs), for the optical information write-in and read-out processes.

The write-in and read-out capabilities of $LiGa_5O_8:Cr^{3+}$ phosphor based on NIR PSPL phenomenon was also visually demonstrated in a deliberate imaging experiment using a night vision monocular. The imaging experiment was carried out on the square $LiGa_5O_8:Cr^{3+}$ ceramic plate in Fig. 2a and lasted for 1,008 h. In the write-in process, the 15 × 15 mm plate with its center covered by an 8 × 8 mm square paper was exposed to a 254 nm UV lamp for 20 min. Due to shielding by the square paper, the center of the plate remained unactivated; thus, the shape of the paper was written on the plate (see Fig. 2b). Under the night vision monocular, the UV-irradiated $LiGa_5O_8:Cr^{3+}$ plate appeared to be a bright square ring, as shown in the NIR image in Fig. 5a. The stored image faded slowly in the dark at room temperature and after 120 h of decay the image can still be clearly seen (Fig. 5a–d). In the decay period of 120–720 h, the right half of the plate was stimulated by a YAG:Ce-based white LED for 20 s at every 120 h (the left half was covered by a piece of paper during the stimulation; the effectiveness of the white LED for the PSPL is given in Supplementary Fig. S4). As expected, only the UV pre-irradiated region on the right half of the plate exhibited enhanced NIR persistent luminescence after each stimulation (Figs. 5e and 5f, and Supplementary Fig. S5a; the PSPL images were taken at 10 s after ceasing the white LED stimulation) and the enhancement lasted for more than 5 h (Fig. 5e1–e3 and Fig. 5f1–f2). In the decay period of 744–1,008 h, the entire plate was exposed to the white LED for 20 s at every 24 h. As a result, the entire UV pre-irradiated region on the plate emitted enhanced NIR persistent luminescence after each stimulation, as shown in the NIR images in Fig. 5g–k (see more images in Supplementary Fig. S5b). Since the left half of the plate received LED stimulations 6 times fewer than the right half (at 744 h, the left half experienced its first stimulation, while the right half received its seventh), the PSPL in the left half is slightly brighter than

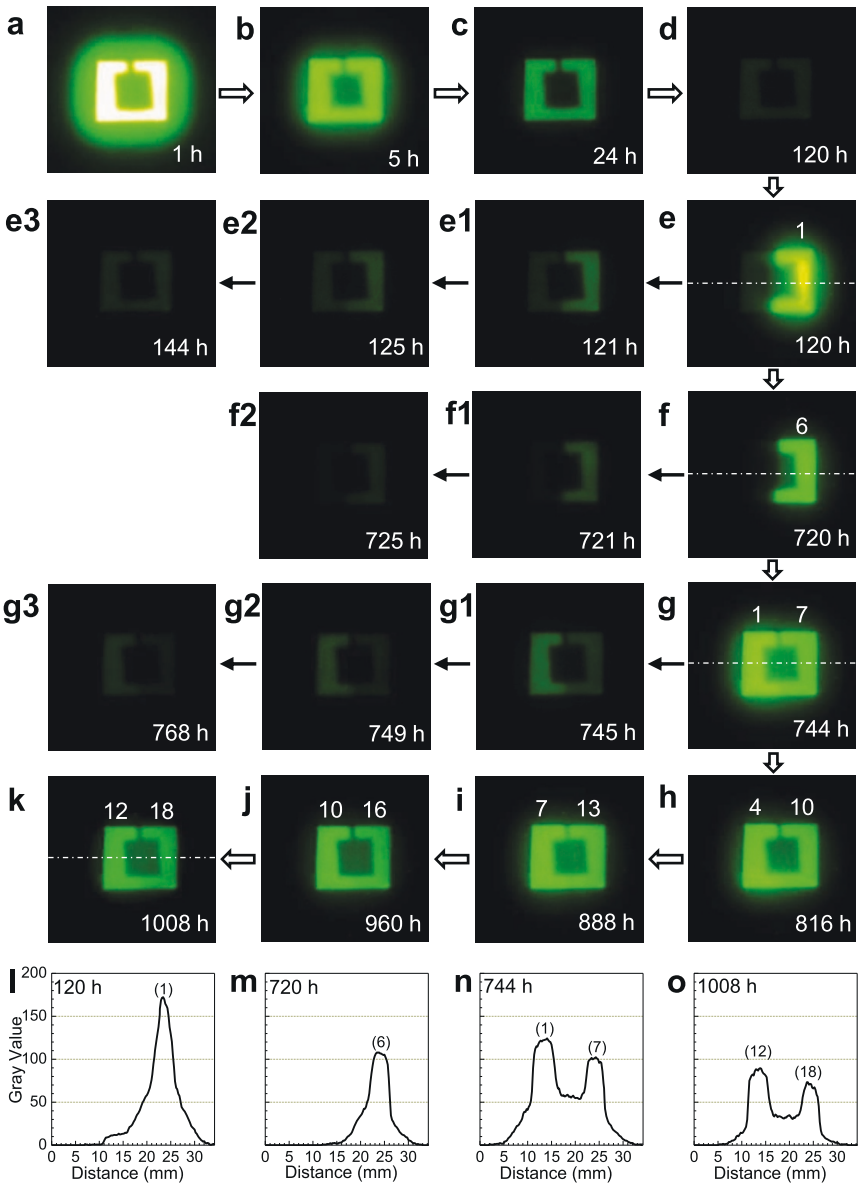

Figure 5 | NIR images for PSPL in $LiGa_5O_8:Cr^{3+}$ phosphor plate. The plate is the same as the one in Fig. 2a. Before imaging the plate was exposed to a 254 nm UV lamp for 20 min. (a–d) Natural decay to 120 h at room temperature. (e–f) From 120 to 720 h, the right half of the plate was stimulated by a white LED for 20 s at every 120 h. (e1–e3) and (f1–f2) show the natural decay after each stimulation. (g–k) From 744 to 1,008 h, the entire plate was stimulated by a white LED for 20 s at every 24 h. (g1–g3) show the natural decay after the stimulation. All the PSPL images were taken at 10 s after ceasing the white LED stimulation. The numbers on the top of the bright square ring in (e–k) are the times of stimulation (i.e., read-out). The imaging parameter is manual/ISO 400/10 s. (i–o) Pixel intensity acquired along the white dot-dash lines in (e), (f), (g), and (k), respectively, by converting each pixel to grayscale using *ImageJ* software. The number on the top of each peak is the times of stimulation.

that in the right half (see also Fig. 5g1–g3). Remarkably, Figure 5k reveals that after 1,008 h of decay and 18 and 12 white LED stimulations on the right half and left half of the plate, respectively, the stored image on the $LiGa_5O_8:Cr^{3+}$ plate can still be clearly read out. (Our prolonged imaging experiments on other samples further showed that the stored information can be clearly read out after even much longer decay, such as 2,000 h, as shown in Supplementary Fig. S6.).

Figure 5e–k also reveals that the PSPL intensity decreases gradually as the read-out times increase due to the photo-release of electrons from the deep traps after each stimulation (the natural decay also contributes to the decrease of PSPL intensity). The decrease of the PSPL intensity can be quantitatively evaluated as pixel intensity by converting each pixel to grayscale using *ImageJ* software[19]. Figure 5i–o shows the pixel intensities acquired from Fig. 5e, Fig. 5f, Fig. 5g, and Fig. 5k, respectively. The dependence of the pixel intensities on the read-out times in Fig. 5i–o is consistent with the visual observation.

Besides the ceramics, we also fabricated $LiGa_5O_8:Cr^{3+}$ phosphor in the form of micro-powders (particle sizes: 2–10 μm) at a lower temperature (1,250°C) by the solid-state reaction method. The powders exhibit similar persistent luminescence and PSPL performances to the ceramics. One advantage of the powder-form phosphor is that the powders can be easily incorporated into paints (for example, transparent acrylic polyurethane vanish) to form NIR persistent luminescent paints which exhibit very good persistent luminescence and PSPL properties, as shown in the NIR images in Supplementary Fig. S7.

Discussion

The above results on PSPL phenomenon in $LiGa_5O_8:Cr^{3+}$ at room temperature indicates that the PSPL write-in process fills the deep

traps with electrons (i.e., forms the photochromic centers), while the PSPL read-out process releases the captured electrons from the filled deep traps (i.e., the photochromic centers) to the conduction band, followed by the refill of the emptied shallow traps. To gain insight into the interaction between the traps and the Cr^{3+} emitting centers, we conducted extended thermoluminescence measurements starting at liquid nitrogen temperature (−196°C, i.e., 77 K) and decay measurement at 77 K on $LiGa_5O_8:Cr^{3+}$ discs, as shown in Fig. 6a and Fig. 6b, respectively. Figure 6a shows two thermoluminescence curves recorded over −196–280°C (i.e., 77–553 K) after irradiating the samples with 300 nm UV light for 20 min at 77 K (dash-line curve) and at room temperature (solid-line curve). (For the case of room-temperature irradiation, the sample was quickly transferred to liquid nitrogen environment for measurement after the stoppage of the irradiation.). In high-temperature region (from room temperature to 280°C), the two curves exhibits the same profile, which is identical in shape to the thermoluminescence curve measured over 20–280°C (the dash-line curve in Fig. 3a). In low-temperature region (from 77 K to room temperature), however, the 77 K pre-irradiated sample shows an additional thermoluminescence band, while the room-temperature pre-irradiated sample does not. This means that there exist low-temperature trap levels in $LiGa_5O_8:Cr^{3+}$, but these low-temperature traps are inactive (i.e., emptied) during room temperature irradiation due to the thermal energy available at room temperature. This trap information indicates that the low-temperature traps will not contribute to the persistent luminescence at 77 K for the samples irradiated at room temperature.

Figure 6b shows a decay curve measured at 77 K for a $LiGa_5O_8:Cr^{3+}$ disc pre-irradiated at room temperature. Before immersing the sample into liquid nitrogen for the measurement, the sample was irradiated by 300 nm light at room temperature for 20 min. The interval between the stoppage of the room-temperature irradiation and the starting of the low-temperature measurement is 120 s. This decay curve was also plotted as a function of reciprocal persistent luminescence intensity versus time, as the linear curve shown in the inset of Fig. 6b. The presence of low-temperature persistent luminescence without the contribution from the low-temperature traps and the linear dependence of the reciprocal persistent luminescence intensity versus time are characteristics of a quantum tunneling process[20,21], meaning that at 77 K the electrons captured in the deep traps can directly recombine with the nearby ionized Cr^{3+} ions via quantum tunneling, instead of going through the conduction band[8]. This tunneling process, which is temperature independent, proceeds at a slow rate, which on the one hand leads to the super-long-persistent luminescence at room temperature, and on the other hand maintains the electron population in the deep traps for a long time for the PSPL process.

Based on the above results and discussions, we propose a mechanism to account for the super-long NIR persistent luminescence and the new NIR PSPL phenomenon at room temperature in $LiGa_5O_8:Cr^{3+}$, as schematically shown in Fig. 6c. To simplify the description, we assign the shallow traps and the filled deep traps (i.e., the photochromic centers) in the PSPL process as TRAP-1 and TRAP-2, respectively. Under UV (250–360 nm) excitation, the ground-state electrons of Cr^{3+} ions are photoionized to the conduction band (process 1). The conduction electrons are subsequently captured by TRAP-1 (process 2) and TRAP-2 (process 3). In the initial stage of the persistent luminescence process, the electrons captured in TRAP-1 escape thermally via the conduction band (process 4) and recombine with the ionized Cr^{3+} ions, which dominates the initial intense persistent NIR emission. Several hours later, the release of electrons through the conduction band can be neglected due to the depletion of TRAP-1. The NIR persistent luminescence subsequently originates mainly from TRAP-2 via quantum tunneling

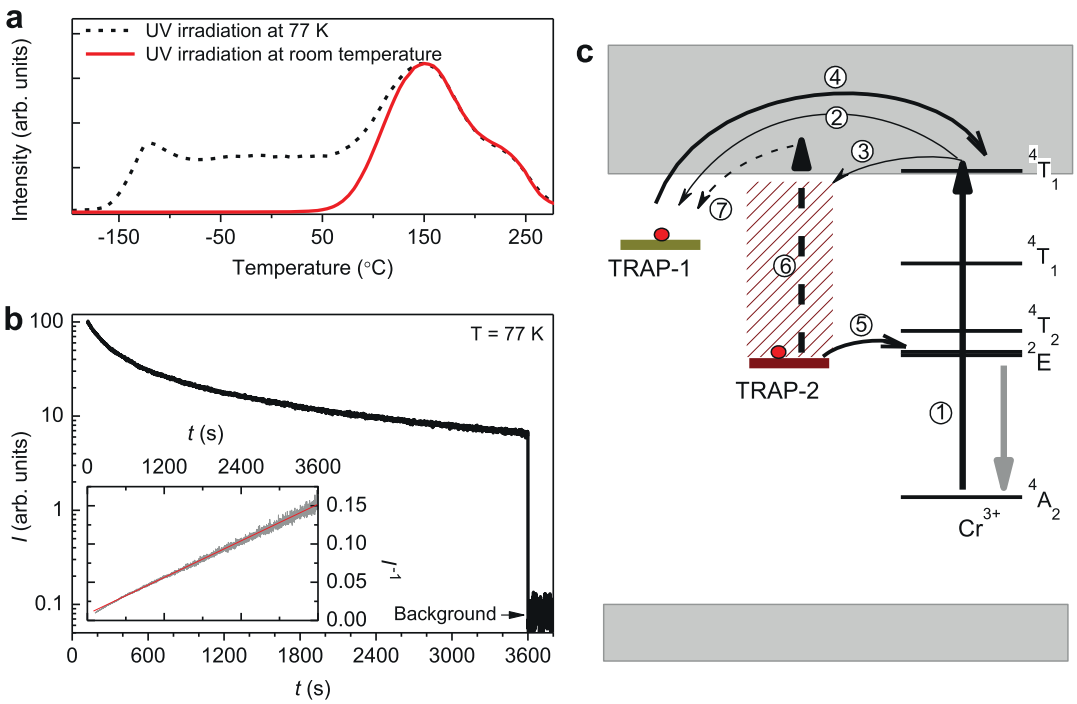

Figure 6 | Low-temperature thermoluminescence and persistent luminescence measurements and NIR PSPL mechanisms in $LiGa_5O_8:Cr^{3+}$. (a) Thermoluminescence curves recorded by monitoring at 716 nm emission over −196–280°C (77–553 K) on a $LiGa_5O_8:Cr^{3+}$ disc. The dash-line curve and solid-line curve were recorded after 300 nm UV light irradiations for 20 min at 77 K and at room temperature, respectively. (b) Persistent luminescence intensity (I) monitored at 716 nm as a function of time (t) at 77 K for a $LiGa_5O_8:Cr^{3+}$ disc pre-irradiated at room temperature. Inset shows the same data plotted as I^{-1} versus t. (c) Schematic representation of the NIR persistent luminescence and photostimulated NIR persistent luminescence mechanisms. The straight-line arrows and curved-line arrows represent optical transition and electron transfer processes (see text for further detail), respectively.

(process 5), giving weak but very-long NIR persistent luminescence. Under the stimulation of a visible or NIR light for a short time at room temperature, some of the electrons in TRAP-2 can be photo-released to the conduction band (process 6) and some of which refill the depleted TRAP-1 (process 7), resulting in enhanced persistent luminescence (i.e., the PSPL phenomenon). Since only some of the electrons in TRAP-2 can be photo-released after photostimulation (owing to short-time, moderate-intensity light stimulation, e.g., a 85-lumen white LED for 20 s in the present study), the PSPL phenomenon can thus occur many times, as the images shown in Fig 5.

The above results show that we have synthesized a novel $LiGa_5O_8:Cr^{3+}$ NIR phosphor that can function as both a self-sustained NIR persistent material exhibiting a super-long (>1,000 h) NIR persistent luminescence and a new type of photostimulable storage material exhibiting repeatedly photostimulated NIR persistent luminescence. This NIR phosphor can be used as a promising storage medium for long-time optical information storage and readout. The material is also expected to be used as invisible (to naked eyes) markers or signage in defense and security[8] and as optical probes in medical diagnosis[22]. Especially, the $LiGa_5O_8:Cr^{3+}$ phosphor in the form of nanoparticles is very suitable for *in vivo* bioimaging because it can avoid some critical inherent problems (e.g., autofluorescence, poor signal-to-noise ratio, and shallow penetration depth) encountered in conventional optical imaging[23–25] owing to the following three key characteristics. Firstly, the material emits intense, long-lasting NIR persistent light after the removal of the excitation. This allows the nanoparticles to be tracked *in vivo* without external excitation, permitting the complete removal of the autofluorescence and hence the background noise originating from *in situ* excitation. The resulting imaging is bestowed with a significantly improved signal-to-noise ratio, allowing for detection in rather deep-tissues with high sensitivity. Secondly, the emission (peaking at 716 nm) is in the tissue transparency window (i.e., in 700–900 nm range)[25], in which light attenuation is largely due to scattering rather than absorption. This can further increase the detection depth. Thirdly, the UV pre-irradiated samples can be repeatedly stimulated by long-wavelength light (e.g., white LED flashlight), which allows for longitudinal (days or even weeks) monitoring/tracking of the $LiGa_5O_8:Cr^{3+}$ labeled cells *in vivo*.

To demonstrate the potential of $LiGa_5O_8:Cr^{3+}$ in *in vivo* bioimaging, we prepared $LiGa_5O_8:Cr^{3+}$ nanoparticles with diameters of 50–150 nm by a sol-gel method followed by high-temperature calcination (Supplementary Fig. S8). The $LiGa_5O_8:Cr^{3+}$ nanoparticles were coated with polyethylenimine (PEI), which were then used to label 4T1 murine breast cancer cells. The PEI-$LiGa_5O_8:Cr^{3+}$ nanoparticles labeled 4T1 cells were illuminated with a 254 nm UV lamp, and subcutaneously injected into the back of a nude mouse. The imaging experiment was performed on an IVIS Lumina II imaging system in the bioluminescence mode for a period of 10 days, as shown in Fig. 7 (the methods used for nanoparticle synthesis, PEI coating, 4T1 cell labeling, and imaging are described in Supplementary Information). The NIR persistent luminescence from the $LiGa_5O_8:Cr^{3+}$ nanoparticles can be clearly imaged even 4 h after the injection (Fig. 7a). As expected, the NIR persistent luminescence can be repeatedly rejuvenated *in vivo* by stimulation with a white LED flashlight (Figs. 7a1–e1), and the resulting PSPL signals can last for more than 5 min (Figs. 7a2–e2). Such repeated NIR PSPL signals permit a wide tracking window and the signals from the $LiGa_5O_8:Cr^{3+}$ nanoparticles can be clearly detected even 10 days after the injection (Fig. 7e1 and 7e2). Similar performance was also observed in a phantom study with PEI-$LiGa_5O_8:Cr^{3+}$ nanoparticles labeled 4T1 cells, as shown in Supplementary Fig. S9.

Methods

Materials synthesis. $LiGa_5O_8:Cr^{3+}$ phosphors in the forms of solid discs and micro-scale powders were synthesized by a solid-state reaction method. Stoichiometric amounts of Li_2CO_3, Ga_2O_3 and Cr_2O_3 powders were ground to form a homogeneous fine powder (the Cr content in the $LiGa_5O_8:Cr^{3+}$ phosphor demonstrated here is 1 atom%). The mixed powder was then prefired at 800°C in air for 2 h. The prefired material was again ground to fine powder suitable for sintering. Part of the prefired powder was pressed into discs with diameters of 15 mm and 40 mm using a 16-ton hydraulic press. The discs were then sintered at 1,300°C in air for 2 h to form a solid ceramic, and the powder samples were sintered at 1,250°C in air for 2 h. The 15-mm-diameter discs were used as-is. Some 40-mm-diameter discs were cut into 15 × 15 mm square plates for deliberate imaging experiments.

$LiGa_5O_8:Cr^{3+}$ phosphor in the forms of nanoparticles was synthesized by a sol-gel method followed by calcination at high temperature. The detailed fabrication procedure is described in Supplementary Information.

Characterization methods. The spectral properties (excitation and emission spectra, decay curves, persistent luminescence emission and excitation spectra, and PSPL write-in and read-out spectra) of the $LiGa_5O_8:Cr^{3+}$ discs were measured using a

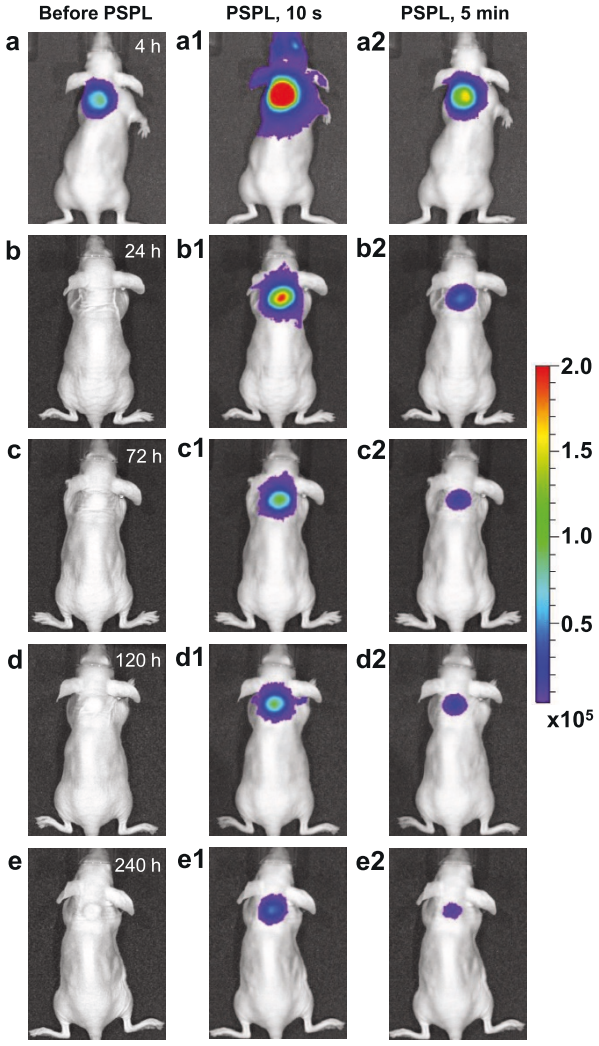

Figure 7 | Images of PEI-$LiGa_5O_8:Cr^{3+}$ nanoparticles labeled 4T1 cells injected into a nude mouse for a 10-day tracking using an IVIS imaging system. The PEI-$LiGa_5O_8:Cr^{3+}$ nanoparticles labeled 4T1 cells (~2.5×10^7 cells) were illuminated by a 4-W 254 nm UV lamp for 15 min, and then subcutaneously injected into the back of a nude mouse. (a) Image taken at 4 h after cell injection. To get the PSPL signal, the mouse was exposed to a white LED flashlight (Olight SR51, 900 lumens) for 15 s. (a1) and (a2), Images taken at 10 s and 5 min after the stimulation, respectively. The signals were attributed to PSPL. (b–e) The mouse was exposed daily to the LED flashlight for 15 s, and images were taken at 10 s and 5 min after the stimulation. All images were acquired in the bioluminescence mode with an exposure time of 2 min. The images were processed using Living Image software at binning of 4 and smooth of 5 × 5. The color scale bar represents the luminescence intensity in the unit of radiance, p/sec/cm^2/sr.

Horiba FluoroLog-3 spectrofluorometer equipped with a 450 W xenon arc lamp and a R928P photomultiplier tube (250–850 nm). All spectra were corrected for the optical system responses. Appropriate optical filters were used to avoid stray light in all spectral measurements. The themoluminescence curves were recorded using a homemade measurement setup (temperature range, −196–280°C; heating rate, 4°C/s). An ITT PVS-14 Generation III night vision monocular was used to monitor the persistent luminescence "brightness" and to take NIR images through a Pentax digital SLR camera connected to the front of the monocular. The monitoring and imaging experiments were conducted in a dark room. Before all the spectral measurements and imaging, the samples were heat-treated in a muffle oven at 400°C for 20 min to completely empty the electron traps.

Four light sources were used to activate the $LiGa_5O_8:Cr^{3+}$ discs/powders for spectral measurements and imaging: a 450 W xenon arc lamp (in a FluoroLog-3 spectrofluorometer), a 4 W 254 nm UV lamp, a 400 mW 980 nm infrared laser, and a YAG:Ce-based white LED flashlight (85 lumens).

The *in vivo* bio-imaging experiments were performed on an IVIS Lumina II imaging system in the bioluminescence mode. A 900-lumen white LED flashlight (Olight SR5) was used as the stimulation source (see Supplementary Information for detail). Animal studies were performed according to a protocol approved by the Institutional Animal Care and Use Committee (IACUC) of University of Georgia.

1. Yukihara, E. G. & McKeever, W. S. *Optically Stimulated Luminescence: Fundamental and Applications* (John Wiley & Sons Ltd., 2011).
2. Schweizer, S. Physics and current understanding of x-ray storage phosphors. *Phys. Stat. Sol. (a)* **187**, 335–393 (2001).
3. Brito, H. F. *et al.* Persistent luminescence mechanism: human imagination at work. *Opt. Mater. Express* **2**, 371–381 (2012).
4. Hölsä, J. Persistent luminescence beats the afterglow: 400 years of persistent luminescence. *Electrochem. Soc. Interface* **18**, 42–45 (2009).
5. van den Eeckhout, K., Smet, P. F. & Poelman, D. Persistent luminescence in Eu^{2+}-doped compounds: a review. *Materials* **3**, 2536–2566 (2010).
6. Matsuzawa, T., Aoki, Y., Takeuchi, N. & Murayama, Y. A new long phosphorescent phosphor with high brightness, $SrAl_2O_4:Eu^{2+},Dy^{3+}$. *J. Electrochem. Soc.* **143**, 2670–2673 (1996).
7. Yamamoto, H. & Matsuzawa, T. Mechanism of long phosphorescence of $SrAl_2O_4:Eu^{2+},Dy^{3+}$ and $CaAl_2O_4:Eu^{2+},Nd^{3+}$. *J. Lumin.* **72**, 287–289 (1997).
8. Pan, Z. W., Lu, Y. Y. & Liu, F. Sunlight-activated long-persistent luminescence in the near-infrared from Cr^{3+}-doped zinc gallogermanates. *Nat. Mater.* **11**, 58–63 (2012).
9. Meijerink, A. & Blasse, G. Photostimulated luminescence and thermally stimulated luminescence of some new x-ray storage phosphors. *J. Phys. D: Appl. Phys.* **24**, 626–632 (1991).
10. von Seggern, H. Photostimulable x-ray storage phosphors: a review of present understanding. *Brazilian J. Phys.* **29**, 254–268 (1999).
11. Riesen, H. & Liu, Z. Q. Optical storage phosphors and materials for ionizing radiation. *Current Topics in Ionizing Radiation Research* (Ed. Nenoi, M.) (InTech, 2012) pp. 625–648.
12. Nanto, H. *et al.* Advanced optical storage phosphor materials for erasable and rewritable optical memory utilizing photostimulated luminescence. *Proc. SPIE* **3802**, 258–265 (1999).
13. Pan, Z. W. & Yan, W. Z. Near infrared doped alkali metal, gallium oxide, alkali metal gallate phosphors. University of Georgia Research Foundation, PCT/US patent application WO 2011/035294 A2 (2011).
14. Szymczak, H., Wardzynska, M. & Mylnikova, I. E. Optical spectrum of Cr^{3+} in the spinel $LiGa_5O_8$. *J. Phys. C: Solid State Phys.* **8**, 3937–3943 (1975).
15. Alig, R. C. Theory of photochromic centers in CaF_2. *Phys. Rev. B* **3**, 536–545 (1971).
16. Staebler, D. L. & Schnatterly, S. E. Optical studies of a photochrominc color center in rare-earth-doped CaF_2. *Phys. Rev. B* **3**, 516–526 (1971).
17. Chandra, V. K. & Chandra, B. P. Dynamics of the mechanoluminescence induced by elastic deformation of persistent luminescent crystals. *J. Lumin.* **132**, 858–869 (2012).
18. Botterman, J. *et al.* Mechanoluminescence in $BaSi_2O_2N_2$:Eu. *Acta Mater.* **60**, 5494–5500 (2012).
19. Schneider, C. A., Rasband, W. S. & Eliceiri, K. W. NIH image to Image *J*: 25 years of image analysis. *Nat. Methods* **9**, 671–675 (2012).
20. Delbecq, C. J., Toyozawa, Y. & Yuster, P. H. Tunneling recombination of trapped electrons and holes in KCl:AgCl and KCl:TlCl. *Phys. Rev. B* **9**, 4497–4505 (1974).
21. Avouris, P. & Morgan, T. N. A tunneling model for the decay of luminescence in inorganic phosphor: the case of Zn_2SiO_4:Mn. *J. Chem. Phys.* **74**, 4347–4355 (1981).
22. de Chermont, Q. L. M. *et al.* Nanoprobes with near-infrared persistent luminescence for *in vivo* imaging. *Proc. Natl. Acad. Sci. USA* **104**, 9266–9271 (2007).
23. Michalet, X. *et al.* Quantum dots for live cells, in vivo imaging, and diagnostics. *Science* **307**, 538–544 (2005).
24. Ntziachristos, V., Bremer, C. & Weissleder, R. Fluorescence imaging with near-infrared light: new technological advances that enable *in vivo* molecular imaging. *Eur. Radiol.* **13**, 195–208 (2003).
25. Frangioni, J. V. In vivo near-infrared fluorescence imaging. *Curr. Opin. Chem. Biol.* **7**, 626–634 (2003).

Acknowledgements

Z.P. acknowledges financial support from the National Science Foundation (CAREER DMR-0955908), the American Chemical Society Petroleum Research Fund (PRF 50265-DN10), and the US Office of Naval Research (N00014-07-1-0060). J.X. acknowledges the support by an NCI/NIH R00 grant (5R00CA153772). We thank John D. Budai for reading the manuscript. We thank Rick Tarleton for allowing us to use the IVIS imaging system.

Author contributions

Z.P. and F.L. conceived and designed the materials synthesis and characterization experiments and wrote the paper. F.L. and W.Y. carried out material synthesis and spectral measurements. F.L. and Z.P. carried out the NIR imaging. F.L. investigated the persistent luminescence mechanism. Y.-J.C. synthesized nanoparticles and analyzed the pixel intensity. J.X. designed the bio-imaging experiments. Y.-J.C., Z.Z. and J.X. carried out bio-imaging experiments. All the authors discussed the results.

Additional information

Supplementary information accompanies this paper at http://www.nature.com/scientificreports

Competing financial interests: The authors declare no competing financial interests.

How to cite this article: Liu, F. *et al.* Photostimulated near-infrared persistent luminescence as a new optical read-out from Cr^{3+}-doped $LiGa_5O_8$. *Sci. Rep.* **3**, 1554; DOI:10.1038/srep01554 (2013).